symmetry

MDPI

Article

Dual-Time-Scale Sliding Mode Control for Surface-Mounted Permanent Magnet Synchronous Motors

Zhiyuan Che [1], Haitao Yu [1,*], Saleh Mobayen [2], Murad Ali [1], Chunyu Yang [3] and Fayez F. M. El-Sousy [4]

1 School of Electrical Engineering, Southeast University, Nanjing 210096, China
2 Multidisciplinary Center for Infrastructure Engineering, Shenyang University of Technology, Shenyang 110870, China
3 School of Information and Control Engineering, China University of Mining and Technology, Xuzhou 221116, China
4 Department of Electrical Engineering, Prince Sattam Bin Abdulaziz University, Al Kharj 16278, Saudi Arabia
* Correspondence: htyu@seu.edu.cn

Abstract: The permanent magnet synchronous motors (PMSMs) as the completely symmetrical three-phase machines, which are usually driven by symmetrical voltage signals. Unfortunately, a PMSM system usually suffers from the different lumped disturbances, such as internal parametric perturbations and external load torques, the speed regulation problem should be addressed within the different operation situations. Characterizing by the current variation speed of the motor winding is much faster than that of the mechanical dynamic velocity, a dual-time-scale sliding mode control (SMC) method for the surface-mounted PMSMs is proposed in this paper. Firstly, the mathematical model of PMSMs is established in the two-phase synchronous rotating orthogonal reference coordinate system, and the slow and fast variation subsystems are obtained based on the quasi-steady-state theory. Secondly, a tracking differentiator (TD)-based and exponential reaching law-based sliding mode controllers are individually designed within dual-time-scale, respectively. As a result, the eventual SMC strategy is presented, and the stability of control system is analyzed by applying the Lyapunov stability theory. The main contribution of this study is to present an alternative control framework for the PMSMs servo system, where the dual-time-scale characteristic is involved, and thus a non-cascade control structure that different from the traditional drive strategy is proposed in the motor community. Finally, the model of whole system is built and carried out on the simulation platform. Research results demonstrate that the presented servo control system can accurately track the reference angle velocity signal, while the strong robustness and fast response performance are guaranteed in the presence of external disturbances. In addition, the three-phase current transient response values are completely symmetrical with the rapid adjustment characteristic.

Keywords: permanent magnet synchronous motors (PMSMs); sliding mode control (SMC); dual-time-scale; symmetrical; Lyapunov stability; tracking differentiator (TD); quasi-steady-state theory

Citation: Che, Z.; Yu, H.; Mobayen, S.; Ali, M.; Yang, C.; El-Sousy, F.F.M. Dual-Time-Scale Sliding Mode Control for Surface-Mounted Permanent Magnet Synchronous Motors. *Symmetry* **2022**, *14*, 1835. https://doi.org/10.3390/sym14091835

Academic Editor: Shyh-Chour Huang

Received: 11 August 2022
Accepted: 2 September 2022
Published: 4 September 2022

1. Introduction

It is well-known that the permanent magnet synchronous motors (PMSMs) will rotate when the symmetrical voltages are applied. Comparing with a DC motor, the three-phase AC PMSMs are characterized by high power factor, small volume, light weight, simple structure, and so on. Therefore, the PMSM servo drive systems have being widely used in high-performance industrial applications [1–6], where require the increasing requirements with fast response, wide speed regulation range and accurate positioning, etc. However, the mathematical model of a PMSM is a nonlinear, high-order and strongly coupled multi-variable system, thus resulting its analysis and design are extremely complex [3]. To this end, it is necessary to simplify the model description, and explore novel control methods [4–6]. Based on the gradient-descent algorithm, an online parameter self-tuning algorithm for

PID control strategy was proposed, and the adaptive speed controller for a PMSM drive system was designed [4]. In literatures [5,6], a robust adaptive sensorless control approach and model predictive servo control system were presented, respectively.

It is well known that the internal parameter perturbations and external disturbances widely exist in almost whole industrial applications, which will inevitably generate the extremely adverse influences on the system performances. In addition, the PMSM drive systems usually operate in different and complex environments, and the corresponding researches should be advocated to address the speed regulation problem. Among the numerous nonlinear control technologies, sliding mode control (SMC) has been extensively receiving much more attention because of simple concept, fast response, powerful robustness and particularly insensitivity to the lumped disturbances [7]. The SMC design procedure is generally comprised by an appropriate sliding mode surface function and a SMC law [8], which should drive the system state variables onto the constructed sliding mode surface in a finite time [9]. After the SMC methodology is applied to the field orientation control (FOC) for a surface-mounted PMSM servo system [10–14], the performance indexes will be characterized by such as rapid dynamic response, strong robustness against various disturbances, etc. In order to reduce the approximation error and improve the PMSM system performance [10], a second-order model was proposed to describe the mathematical relationship between the quadrature axis reference current and the speed output. In literatures [11,12], the extended state observer (ESO) and a DO were separately designed to estimate the parameter perturbations and external disturbances, respectively, and their estimation values were incorporated into the design of terminal SMC laws. In addition, a generalized proportional integral observer (GPIO)-based sliding mode speed regulation system was presented in [13]. A novel reaching law-based SMC approach was implemented in [14], where an extended sliding mode disturbance observer characterized by the low pass filter (LPF) was proposed and analyzed to accurately compensate the lumped uncertainties. However, it is worth mentioning that the above mentioned approaches essentially concentrate on the design and improvement of the speed loop [10–14], which belongs to the conventional double closed-loop vector control structure.

By involving the extended high gain observer [15], the uncertain dynamics terms were accurately estimated for compensation purpose, which were incorporated into the proposed output feedback controller for reconfigurable pavement sweeping wheeled mobile robots. Based on the nonlinear disturbance observer (DO) and feedback linearization technology, a speed-current single-loop SMC control strategy for a PMSM drive system was proposed [16]. The dual DOs-based single loop non-cascade integral SMC was presented to simplify the control framework [17], while the uncertainties and disturbances were considered by employing the similar composite structure [2]. However, there still required an individual PI controller for direct axis current regulation [2,17]. It should be emphasized that the above mentioned non-cascade control framework is also an alternative and effective way to regulate a PMSM drive system, which usually differentiates from the traditional cascade control structure. On the other hand, in order to improve the speed regulation performance, the frequency of outer speed loop is usually designed smaller than that of inner current loop in a conventional dual closed-loop vector control framework, which provides a favorable guideline to the well-known PI engineering parameter determinations. As mentioned in [10], the torque/current was controlled with a response time faster than that of the speed, thus resulting the large control period difference between the speed and current loops. Meanwhile, the dual reduced-order PI observer-based robust cascade control for a DC motor drive system was proposed in [18], where the closed-loop transfer function for each loop was characterized by a classical inertia element. Moreover, the bandwidth of the current loop was chosen much larger than that of the outer-loop system in the design of cascade control scheme, and then the singular perturbation theory was presented to analyze the augmented system. It is worth mentioning that singular perturbation approach as a powerful tool, has being widely employed in considerable industrial applications [18–23]. The output feedback control for a single link manipulator was presented in [19], which was modeled as an uncertain singularly perturbed system. For the 90th-order advanced heavy water reactor spatial stabilization system [20], the singularly perturbed three-time-scale method was introduced to reduce the design complexity and computational time. The continuous SMC for compliant robot arms was regarded as a singularly perturbed system comprising by a slow rigid robot and the fast series elastic actuator dynamics [21], such achieving high-precision tracking performance. From the above discussions, it can be concluded that a PMSM drive system has the obvious time-scale characteristic, and thus it is feasible to employ the singularly perturbed approach. To our best knowledge, the electrical transients are rather fast comparing with the mechanical response, which is also characterized by the large time constant difference. To this end, according to the singular perturbation theory, a PMSM servo system is a typical dual-time-scale system [22]. As a result, by employing quasi-steady-state decomposing theory, the original full-order mathematical models of a surface-mounted PMSM can be approximately equivalent to slow variation subsystem (namely, quasi-steady equation) and fast variation subsystem (i.e., boundary layer system) within slow- and fast-time scales, respectively [23]. Therefore, it is an effective and alternative method to promote the control performance of a PMSM servo system by individually designing controllers in different time-scales, where the powerful SMC technique can be adopted to stabilize the decoupled subsystems and improve the anti-disturbance ability. However, there has few reported literatures in this research direction, which is of important significance to motor control community.

By incorporating the disturbance estimation value provided by an improved extended state observer into the feedback control law [3], we have devoted ourselves to conducting the corresponding research on a PMSM speed regulation problem. Motivated by the above discussions, this study firstly establishes the mathematical model of a surface-mounted PMSM in the two-phase synchronous rotating orthogonal reference coordinate system, and then its state-space equation is subsequently obtained. By adopting the quasi-steady-state theory-based decoupling approach, the slow and fast variation subsystems are derived within slow-time-scale and fast-time-scale, respectively. In order to incorporate the differential signal into the controller design, a tracking differentiator (TD)-based SMC law is presented for the slow variation subsystem. Meanwhile, taking the exponential reaching law into account, another sliding mode controller is proposed to stabilize the fast variation subsystem. As a result, the eventual SMC strategy is synthesized, and the stability of closed-loop system is analyzed by applying the Lyapunov stability theory. Finally, the model of whole system is built and carried out on the Matlab/Simulink platform. Research results can demonstrate the effectiveness of the presented servo control system and robustness against disturbances. The contributions of this study can be summarized as follows. (1) The quasi-steady dynamics and boundary layer system are individually obtained by the singular perturbation decomposition theory, which are characterized by dual-time-scale feature. (2) An alternative control framework for the PMSMs servo system is presented based on the SMC technology, which is different from the traditional cascade drive strategy. (3) The employed TD can generate the favorable transition dynamic and high quality differential signal, simultaneously, such improving system performance of the presented control method.

The rest of this paper is organized as follows. In Section 2, dual-time-scale system modeling and preliminaries are presented. The main results are given in Section 3, including the design and analysis of the individual and eventual controllers in details. Some simulation results are prsented in Section 4. Section 5 concludes this paper.

2. Dual-Time-Scale System Modeling and Preliminaries

In the three-phase symmetrical static $A-B-C$ reference coordinate system, the mathematical model of a PMSM is composed by voltage, flux linkage, electromagnetic torque and motion equations, which are strongly coupled and nonlinear [4]. According to the well-known Clark and Park transformations, the general dynamic model of a surface-mounted

PMSM can be established with respect to two-phase synchronous rotating orthogonal $d-q$ coordinate system [14], which is comprised by electrical dynamics

$$\begin{cases} L_{\mathrm{s}}\frac{\mathrm{d}}{\mathrm{d}t}i_{\mathrm{d}} = u_{\mathrm{d}} - R_{\mathrm{s}}i_{\mathrm{d}} + \omega_{\mathrm{e}}L_{\mathrm{s}}i_{\mathrm{q}} \\ L_{\mathrm{s}}\frac{\mathrm{d}}{\mathrm{d}t}i_{\mathrm{q}} = u_{\mathrm{q}} - R_{\mathrm{s}}i_{\mathrm{q}} - \omega_{\mathrm{e}}L_{\mathrm{s}}i_{\mathrm{d}} - \omega_{\mathrm{e}}\psi_{\mathrm{f}} \end{cases} \tag{1}$$

and mechanical dynamic equation

$$J\frac{\mathrm{d}}{\mathrm{d}t}\omega_{\mathrm{m}} = K_{\mathrm{T}}i_{\mathrm{q}} - F\omega_{\mathrm{m}} - T_{\mathrm{m}} \tag{2}$$

where L_{s} is the stator inductance; i_{d} and i_{q} denote d and q axes stator currents, respectively; u_{d} and u_{q} represent d and q axes stator voltages, respectively; R_{s} is stator resistance; ψ_{f} is the flux linkage of permanent magnets; J is the moment of the rotational inertia; $K_{\mathrm{T}} = 3p_{\mathrm{n}}\psi_{\mathrm{f}}/2$ is the electromagnetic torque coefficient, and p_{n} is the number of pole pairs; F is the viscous friction coefficient; T_{m} represents the load torque disturbance, which characterizing by $\dot{T}_{\mathrm{m}} = 0$; ω_{e} and ω_{m} are electrical and mechanical angular velocities, respectively, which satisfying $\omega_{\mathrm{e}} = p_{\mathrm{n}}\omega_{\mathrm{m}}$.

Remark 1. *Based on the above mentioned mathematical model (1) and (2), the traditional cascade servo controller design of a PMSM drive system belongs to a double closed-loop vector control structure [10–14], which benefits form the large bandwidth difference between the outer speed and inner current loops. If we consider the characteristic of their time constants and take them into account, a typical dual-time-scale system can be easily modeled. However, it is still an open research direction, and there has few reported literatures in this field.*

Introduce the state vector and control input as

$$\boldsymbol{i} = \begin{bmatrix} i_{\mathrm{d}} \\ i_{\mathrm{q}} \end{bmatrix}, \qquad \boldsymbol{u} = \begin{bmatrix} u_{\mathrm{d}} \\ u_{\mathrm{q}} \end{bmatrix} \tag{3}$$

And then substituting the above definitions (3) into the mathematical Equations (1) and (2), thus resulting their following state space description form:

$$\begin{cases} \frac{\mathrm{d}}{\mathrm{d}t}\boldsymbol{i} = \begin{bmatrix} -\frac{R_{\mathrm{s}}}{L_{\mathrm{s}}} & \omega_{\mathrm{e}} \\ -\omega_{\mathrm{e}} & -\frac{R_{\mathrm{s}}}{L_{\mathrm{s}}} \end{bmatrix}\boldsymbol{i} + \frac{1}{L_{\mathrm{s}}}\boldsymbol{u} - \begin{bmatrix} 0 \\ \frac{\psi_{\mathrm{f}}}{L_{\mathrm{s}}}\omega_{\mathrm{e}} \end{bmatrix} \\ \frac{\mathrm{d}}{\mathrm{d}t}\omega_{\mathrm{m}} = -\frac{F}{J}\omega_{\mathrm{m}} + \begin{bmatrix} 0 & \frac{K_{\mathrm{T}}}{J} \end{bmatrix}\boldsymbol{i} - \frac{1}{J}T_{\mathrm{m}} \end{cases} \tag{4}$$

The objective of this study is to design the eventual SMC law $\boldsymbol{u}$ for a surface-mounted PMSM (4), such that the mechanical angular velocity ω_{m} should be accurately regulated to its reference velocity value ω_{m}^* in the presences of the external disturbances.

To our best knowledge, the electrical transients (namely, currents i_{d} and i_{q}) are rather fast comparing with the mechanical response (i.e., angular velocity ω_{m}) [10], which can be also characterized by

$$T_{\mathrm{c}} \ll T_{\mathrm{s}} \tag{5}$$

where $T_{\mathrm{c}} = L_{\mathrm{s}}/R_{\mathrm{s}}$ and $T_{\mathrm{s}} = J/F$ denote the electrical and mechanical time constants, respectively.

According to the above relationship, it can be concluded that the PMSM is an typical dual-time-scale system [23]. As a result, a singularly perturbed system can be derived by choosing the singular perturbation parameter as

$$\varepsilon = T_{\mathrm{c}} \tag{6}$$

And then, the Formulation (4) can be modeled as

$$\begin{cases} \frac{\mathrm{d}}{\mathrm{d}t}\omega_{\mathrm{m}} = -\frac{F}{J}\omega_{\mathrm{m}} + \begin{bmatrix} 0 & \frac{K_{\mathrm{T}}}{J} \end{bmatrix}\boldsymbol{i} - \frac{1}{J}T_{\mathrm{m}} \\ \varepsilon\frac{\mathrm{d}}{\mathrm{d}t}\boldsymbol{i} = \begin{bmatrix} -1 & \frac{p_{\mathrm{n}}L_{\mathrm{s}}}{R_{\mathrm{s}}}\omega_{\mathrm{m}} \\ -\frac{p_{\mathrm{n}}L_{\mathrm{s}}}{R_{\mathrm{s}}}\omega_{\mathrm{m}} & -1 \end{bmatrix}\boldsymbol{i} + \frac{1}{R_{\mathrm{s}}}\boldsymbol{u} - \begin{bmatrix} 0 \\ \frac{p_{\mathrm{n}}\psi_{\mathrm{f}}}{R_{\mathrm{s}}}\omega_{\mathrm{m}} \end{bmatrix} \end{cases} \tag{7}$$

According to the quasi-steady-state theory [21], one can firstly set $\varepsilon = 0$, thus resulting the following equations:

$$\begin{cases} \frac{\mathrm{d}}{\mathrm{d}t}\omega_{\mathrm{ms}} = -\frac{F}{J}\omega_{\mathrm{ms}} + \begin{bmatrix} 0 & \frac{K_{\mathrm{T}}}{J} \end{bmatrix}\boldsymbol{i}_{\mathrm{s}} - \frac{1}{J}T_{\mathrm{m}} \\ 0 = \begin{bmatrix} -1 & \frac{p_{\mathrm{n}}L_{\mathrm{s}}}{R_{\mathrm{s}}}\omega_{\mathrm{ms}} \\ -\frac{p_{\mathrm{n}}L_{\mathrm{s}}}{R_{\mathrm{s}}}\omega_{\mathrm{ms}} & -1 \end{bmatrix}\boldsymbol{i}_{\mathrm{s}} + \frac{1}{R_{\mathrm{s}}}\boldsymbol{u}_{\mathrm{s}} - \begin{bmatrix} 0 \\ \frac{p_{\mathrm{n}}\psi_{\mathrm{f}}}{R_{\mathrm{s}}}\omega_{\mathrm{ms}} \end{bmatrix} \end{cases} \tag{8}$$

where the extra subscript "s" represents the slow variable components (namely, quasi-steady-states) of the corresponding physical quantities (including the angular velocity, currents and voltages).

According to the Formulation (5), the change of mechanical angular velocity is significantly slower than that of currents and voltages. To this end, it is feasible to assume that $\omega_{\mathrm{m}} = \omega_{\mathrm{ms}}$ within the slow-time-scale t. As a result, the solution of the quasi-steady-state Equation (8) can be calculated as follows

$$\boldsymbol{i}_{\mathrm{s}} = \frac{1}{N(\omega_{\mathrm{m}})}\begin{bmatrix} 1 & \frac{p_{\mathrm{n}}L_{\mathrm{s}}}{R_{\mathrm{s}}}\omega_{\mathrm{m}} \\ -\frac{p_{\mathrm{n}}L_{\mathrm{s}}}{R_{\mathrm{s}}}\omega_{\mathrm{m}} & 1 \end{bmatrix}\left(\frac{1}{R_{\mathrm{s}}}\boldsymbol{u}_{\mathrm{s}} - \begin{bmatrix} 0 \\ \frac{p_{\mathrm{n}}\psi_{\mathrm{f}}}{R_{\mathrm{s}}}\omega_{\mathrm{m}} \end{bmatrix}\right) \tag{9}$$

where $N(\omega_{\mathrm{m}}) = 1 + \left(p_{\mathrm{n}}L_{\mathrm{s}}\omega_{\mathrm{m}}/R_{\mathrm{s}}\right)^2$.

Combining (8) with (9), the following slow variation subsystem can be obtained:

$$\frac{\mathrm{d}}{\mathrm{d}t}\omega_{\mathrm{m}} = -\left(\frac{F}{J} + \frac{p_{\mathrm{n}}K_{\mathrm{T}}\psi_{\mathrm{f}}}{JR_{\mathrm{s}}N(\omega_{\mathrm{m}})}\right)\omega_{\mathrm{m}} + \frac{K_{\mathrm{T}}}{JR_{\mathrm{s}}N(\omega_{\mathrm{m}})}\begin{bmatrix} -\frac{p_{\mathrm{n}}L_{\mathrm{s}}}{R_{\mathrm{s}}}\omega_{\mathrm{m}} & 1 \end{bmatrix}\boldsymbol{u}_{\mathrm{s}} - \frac{1}{J}T_{\mathrm{m}} \tag{10}$$

On the other hand, one can introduce the following fast-time-scale:

$$\tau = \frac{t}{\varepsilon} \tag{11}$$

Then, the derivatives of the corresponding physical quantities indicated by subscript "s" in slow variation subsystem (10) are equal to zero within this fast-time scale τ. By combining (7) with (9) and (11), the fast variation subsystem can be derived as follows

$$\frac{\mathrm{d}}{\mathrm{d}\tau}\boldsymbol{i}_{\mathrm{f}} = \begin{bmatrix} -1 & \frac{p_{\mathrm{n}}L_{\mathrm{s}}}{R_{\mathrm{s}}}\omega_{\mathrm{m}} \\ -\frac{p_{\mathrm{n}}L_{\mathrm{s}}}{R_{\mathrm{s}}}\omega_{\mathrm{m}} & -1 \end{bmatrix}\boldsymbol{i}_{\mathrm{f}} + \frac{1}{R_{\mathrm{s}}}\boldsymbol{u}_{\mathrm{f}} \tag{12}$$

where the extra subscript "f" denotes the fast variable components (namely, boundary layer states) of the above mentioned corresponding physical quantities, which satisfying $\boldsymbol{i}_{\mathrm{f}} = \boldsymbol{i} - \boldsymbol{i}_{\mathrm{s}}$ and $\boldsymbol{u}_{\mathrm{f}} = \boldsymbol{u} - \boldsymbol{u}_{\mathrm{s}}$, respectively.

From (10) and (12), it can be concluded that the mathematical model of a surface-mounted PMSM can be eventually described as the following slow variation subsystem:

$$\frac{\mathrm{d}}{\mathrm{d}t}\omega_{\mathrm{m}} = -\left(\frac{F}{J} + \frac{p_{\mathrm{n}}K_{\mathrm{T}}\psi_{\mathrm{f}}}{JR_{\mathrm{s}}N(\omega_{\mathrm{m}})}\right)\omega_{\mathrm{m}} + \frac{K_{\mathrm{T}}}{JR_{\mathrm{s}}N(\omega_{\mathrm{m}})}\begin{bmatrix} -\frac{p_{\mathrm{n}}L_{\mathrm{s}}}{R_{\mathrm{s}}}\omega_{\mathrm{m}} & 1 \end{bmatrix}\boldsymbol{u}_{\mathrm{s}} - \frac{1}{J}T_{\mathrm{m}} \tag{13}$$

and the fast variation subsystem as follows

$$\frac{\mathrm{d}}{\mathrm{d}\tau}\boldsymbol{i}_{\mathrm{f}} = \begin{bmatrix} -1 & \frac{p_{\mathrm{n}}L_{\mathrm{s}}}{R_{\mathrm{s}}}\omega_{\mathrm{m}} \\ -\frac{p_{\mathrm{n}}L_{\mathrm{s}}}{R_{\mathrm{s}}}\omega_{\mathrm{m}} & -1 \end{bmatrix}\boldsymbol{i}_{\mathrm{f}} + \frac{1}{R_{\mathrm{s}}}\boldsymbol{u}_{\mathrm{f}} \tag{14}$$

Remark 2. *According to the quasi-steady-state theory, the original full-order mathematical descriptions (1) and (2) can be approximately decomposed into the above mentioned slow and fast variation subsystems. Therefore, a eventual SMC law can be synthesized by individually designing corresponding controllers in slow-time-scale t and fast-time-scale τ, respectively.*

3. SMC Design and Analysis

In this section, we will design and analyze the controller $\boldsymbol{u}$ for a surface-mounted PMSM, which includes SMC laws $\boldsymbol{u}_\mathrm{s}$ and $\boldsymbol{u}_\mathrm{f}$ for decoupled slow and fast variation subsystems, respectively.

3.1. A TD-Based SMC Design for Slow Variation Subsystem

According to (13), the slow variation subsystem of the surface-mounted PMSM can be rewritten as follows

$$\frac{\mathrm{d}}{\mathrm{d}t}\omega_\mathrm{m} = A_\mathrm{s}\omega_\mathrm{m} + \boldsymbol{B}_\mathrm{s}\boldsymbol{u}_\mathrm{s} - \frac{1}{J}T_\mathrm{m} \tag{15}$$

with the following parameter definitions:

$$A_\mathrm{s} = -\left(\frac{F}{J} + \frac{p_\mathrm{n}K_\mathrm{T}\psi_\mathrm{f}}{JR_\mathrm{s}N(\omega_\mathrm{m})}\right), \qquad \boldsymbol{B}_\mathrm{s} = \frac{K_\mathrm{T}}{JR_\mathrm{s}N(\omega_\mathrm{m})}\begin{bmatrix} -\frac{p_\mathrm{n}L_\mathrm{s}}{R_\mathrm{s}}\omega_\mathrm{m} & 1 \end{bmatrix} \tag{16}$$

We can introduce the following velocity tracking error:

$$e_\mathrm{w} = \omega_\mathrm{m}^* - \omega_\mathrm{m} \tag{17}$$

And then, a linear slow variable sliding mode surface function can be constructed as follows

$$S_\mathrm{s} = ce_\mathrm{w} + \dot{e}_\mathrm{w} \tag{18}$$

where $c > 0$ is the tracking error coefficient.

Calculating the time-derivative of the S_s in terms of e_w, leads to

$$\dot{S}_\mathrm{s} = c\dot{e}_\mathrm{w} + \ddot{\omega}_\mathrm{m}^* - \ddot{\omega}_\mathrm{m} = c\dot{e}_\mathrm{w} + \ddot{\omega}_\mathrm{m}^* - A_\mathrm{s}\dot{\omega}_\mathrm{m} - \boldsymbol{B}_\mathrm{s}\dot{\boldsymbol{u}}_\mathrm{s} \tag{19}$$

Based on the exponential reaching law [13], a slow-SMC (S-SMC) can be designed as follows

$$\boldsymbol{u}_\mathrm{s} = \begin{bmatrix} u_\mathrm{ds} \\ u_\mathrm{qs} \end{bmatrix} = \int_0^t \frac{JR_\mathrm{s}}{K_\mathrm{T}}\begin{bmatrix} -\frac{p_\mathrm{n}L_\mathrm{s}}{R_\mathrm{s}}\omega_\mathrm{m} \\ 1 \end{bmatrix}(c\dot{e}_\mathrm{w} + \ddot{\omega}_\mathrm{m}^* - A_\mathrm{s}\dot{\omega}_\mathrm{m} + \xi_\mathrm{s}\mathrm{sgn}(S_\mathrm{s}) + k_\mathrm{s}S_\mathrm{s})\mathrm{d}t \tag{20}$$

where sgn $(\cdot)$ denotes the sign function; $\xi_\mathrm{s} > 0$ and $k_\mathrm{s} > 0$ represent the slow switching and exponential gains, respectively.

For the above mentioned controller (20), there need the differential operation for the some signals. The traditional backward difference (BD)-based extraction method will inevitably confront and amplify the measurement noise [24]. At the same time, for the purpose of promoting the tracking performance, it is recommended to arrange the smooth transition dynamic for the reference velocity value, which is commonly given as a step signal. In order to realize the above mentioned objectives, an optimal control synthesis function-based TD is presented in this section, which is aimed at providing a transition signal, while the first and second-order differential information are feasible to S-SMC (20), simultaneously. For the following continuous system:

$$\begin{bmatrix} \dot{x}_1 \\ \dot{x}_2 \end{bmatrix} = \begin{bmatrix} x_2 \\ u_\mathrm{r} \end{bmatrix} \tag{21}$$

where $|u_r| \leq r$, and r is the velocity factor.

An optimal nonlinear function is employed for its discrete-time system, yields the following nonlinear TD:

$$\begin{bmatrix} \hat{x}_1(k+1) - \hat{x}_1(k) \\ \hat{x}_2(k+1) - \hat{x}_2(k) \end{bmatrix} = T_o \begin{bmatrix} \hat{x}_2(k) \\ \text{fhan}(e(k), \hat{x}_2(k), r, h) \end{bmatrix} \tag{22}$$

where $\hat{x}_1$ and $\hat{x}_2$ are the real-time estimation values for x_1 and its differential signal x_2, respectively; T_o is the discrete step; k and $k+1$ represent the current and next instants, respectively; $e(k) = \hat{x}_1(k) - x_1(k)$ is the tracking error; h is the filtering factor [25].

The optimal control synthesis function $u_r = \text{fhan}(\cdot)$ is summarized as follows

$$\begin{aligned} d &= rh, \quad d_o = hd \\ y &= e(k) + h\hat{x}_2(k) \\ a_o &= \sqrt{d^2 + 8r|y|} \\ a &= \begin{cases} \hat{x}_2(k) + \frac{a_o - d}{2}\text{sgn}(y), & |y| > d_o \\ \hat{x}_2(k) + \frac{y}{h}, & |y| \leq d_o \end{cases} \\ \text{fhan}(e(k), \hat{x}_2(k), r, h) &= -\begin{cases} r\text{sgn}(a), & |a| > d \\ r\frac{a}{d}, & |a| \leq d \end{cases} \end{aligned} \tag{23}$$

Remark 3. *The exhibited high performance TD (22) has strong insensitivity to the parameter perturbations of r and h. A large value of the speed factor r will decrease the response time of the transition tracking dynamic. Meanwhile, a smaller discrete step T_o is beneficial to suppress noise influence. In addition, the filtering factor h should be selected greater than the value of T_o, which determines the noise attenuation characteristic. In a summary, when choosing the appropriate parameters values for presented TD (22), there should adequately take the tracking and filtering performances into account.*

Remark 4. *It is worth mentioning that the above mentioned design procedure of TD (22) is directly implemented in the discrete-time domain, thus greatly improving feasibility and realizability of the proposed strategy for the actual industrial applications.*

3.2. SMC Design for Fast Variation Subsystem

According to (14), the fast variation subsystem of the surface-mounted PMSM can be rewritten as follows

$$\frac{\mathrm{d}}{\mathrm{d}\tau}\boldsymbol{i}_f = \boldsymbol{A}_f\boldsymbol{i}_f + \frac{1}{R_s}\boldsymbol{u}_f \tag{24}$$

with the following parameter matrix:

$$\boldsymbol{A}_f = \begin{bmatrix} -1 & \frac{p_n L_s}{R_s}\omega_m \\ -\frac{p_n L_s}{R_s}\omega_m & -1 \end{bmatrix} \tag{25}$$

A linear fast variable sliding mode surface function can be constructed as follows

$$\boldsymbol{S}_f = \begin{bmatrix} S_{df} \\ S_{qf} \end{bmatrix} = \begin{bmatrix} i_{df} \\ i_{qf} \end{bmatrix} = \boldsymbol{i}_f \tag{26}$$

Calculating the time-derivative of the $\boldsymbol{S}_f$ in terms of $\boldsymbol{i}_f$, leads to

$$\dot{\boldsymbol{S}}_f = \frac{\mathrm{d}}{\mathrm{d}\tau}\boldsymbol{i}_f = \boldsymbol{A}_f\boldsymbol{i}_f + \frac{1}{R_s}\boldsymbol{u}_f \tag{27}$$

Based on the exponential reaching law [13], a fast-SMC (F-SMC) can be designed as follows

$$\boldsymbol{u}_{\mathrm{f}} = \begin{bmatrix} u_{\mathrm{df}} \\ u_{\mathrm{qf}} \end{bmatrix} = -R_{\mathrm{s}}(\boldsymbol{A}_{\mathrm{f}}\boldsymbol{i}_{\mathrm{f}} + \xi_{\mathrm{f}}\mathrm{sgn}(\boldsymbol{S}_{\mathrm{f}}) + k_{\mathrm{f}}\boldsymbol{S}_{\mathrm{f}}) \tag{28}$$

where $\xi_{\mathrm{f}} > 0$ and $k_{\mathrm{f}} > 0$ represent the fast switching and exponential gains, respectively.

3.3. Eventual SMC Design and Analysis

According to the quasi-steady-state theory [21], the eventual SMC law can be synthesized by combining (20) and (28), that is to say

$$\begin{aligned} \boldsymbol{u} = \boldsymbol{u}_{\mathrm{s}} + \boldsymbol{u}_{\mathrm{f}} &= \begin{bmatrix} u_{\mathrm{ds}} \\ u_{\mathrm{qs}} \end{bmatrix} + \begin{bmatrix} u_{\mathrm{df}} \\ u_{\mathrm{qf}} \end{bmatrix} \\ &= \int_0^t \frac{JR_{\mathrm{s}}}{K_{\mathrm{T}}} \begin{bmatrix} -\frac{p_{\mathrm{n}}L_{\mathrm{s}}}{R_{\mathrm{s}}}\omega_{\mathrm{m}} \\ 1 \end{bmatrix} (c\dot{e}_{\mathrm{w}} + \ddot{\omega}_{\mathrm{m}}^{*} - A_{\mathrm{s}}\dot{\omega}_{\mathrm{m}} + \xi_{\mathrm{s}}\mathrm{sgn}(S_{\mathrm{s}}) + k_{\mathrm{s}}S_{\mathrm{s}})\mathrm{d}t - \\ &\quad R_{\mathrm{s}}(\boldsymbol{A}_{\mathrm{f}}\boldsymbol{i}_{\mathrm{f}} + \xi_{\mathrm{f}}\mathrm{sgn}(\boldsymbol{S}_{\mathrm{f}}) + k_{\mathrm{f}}\boldsymbol{S}_{\mathrm{f}}) \end{aligned} \tag{29}$$

For the proposed SMC (29), we have the following theorem.

Theorem 1. *The controlled system under the SMC (29) is asymptotically stable. Namely, The system state variables will uniformly converge their equilibrium points, respectively.*

Proof. First of all, we can construct the following sliding mode surface function:

$$\boldsymbol{S} = \begin{bmatrix} S_{\mathrm{s}} \\ \boldsymbol{S}_{\mathrm{f}} \end{bmatrix} \tag{30}$$

Introducing the Lyapunov candidate function as the following quadratic form:

$$V(\boldsymbol{S}) = \frac{\boldsymbol{S}^{\mathrm{T}}\boldsymbol{S}}{2} = \frac{S_{\mathrm{s}}^2 + \boldsymbol{S}_{\mathrm{f}}^{\mathrm{T}}\boldsymbol{S}_{\mathrm{f}}}{2} \tag{31}$$

Calculating the time-derivative of the $V(\boldsymbol{S})$ in terms of $\boldsymbol{S}$, while taking the first-order differential descriptions of sliding mode surface (19) and (27) into account, yield

$$\begin{aligned} \dot{V}(\boldsymbol{S}) &= S_{\mathrm{s}}\dot{S}_{\mathrm{s}} + \boldsymbol{S}_{\mathrm{f}}^{\mathrm{T}}\dot{\boldsymbol{S}}_{\mathrm{f}} = S_{\mathrm{s}}[c\dot{e}_{\mathrm{w}} + \ddot{\omega}_{\mathrm{m}}^{*} - A_{\mathrm{s}}\dot{\omega}_{\mathrm{m}} - \boldsymbol{B}_{\mathrm{s}}\dot{\boldsymbol{u}}_{\mathrm{s}}] + \boldsymbol{S}_{\mathrm{f}}^{\mathrm{T}}\left[\boldsymbol{A}_{\mathrm{f}}\boldsymbol{i}_{\mathrm{f}} + \frac{1}{R_{\mathrm{s}}}\boldsymbol{u}_{\mathrm{f}}\right] \\ &= S_{\mathrm{s}}\left\{c\dot{e}_{\mathrm{w}} + \ddot{\omega}_{\mathrm{m}}^{*} - A_{\mathrm{s}}\dot{\omega}_{\mathrm{m}} - \frac{JR_{\mathrm{s}}\boldsymbol{B}_{\mathrm{s}}}{K_{\mathrm{T}}}\begin{bmatrix} -\frac{p_{\mathrm{n}}L_{\mathrm{s}}}{R_{\mathrm{s}}}\omega_{\mathrm{m}} \\ 1 \end{bmatrix}(c\dot{e}_{\mathrm{w}} + \ddot{\omega}_{\mathrm{m}}^{*} - A_{\mathrm{s}}\dot{\omega}_{\mathrm{m}} + \xi_{\mathrm{s}}\mathrm{sgn}(S_{\mathrm{s}}) + k_{\mathrm{s}}S_{\mathrm{s}})\right\} + \\ &\quad \boldsymbol{S}_{\mathrm{f}}^{\mathrm{T}}[\boldsymbol{A}_{\mathrm{f}}\boldsymbol{i}_{\mathrm{f}} - (\boldsymbol{A}_{\mathrm{f}}\boldsymbol{i}_{\mathrm{f}} + \xi_{\mathrm{f}}\mathrm{sgn}(\boldsymbol{S}_{\mathrm{f}}) + k_{\mathrm{f}}\boldsymbol{S}_{\mathrm{f}})] \\ &= -\xi_{\mathrm{s}}|S_{\mathrm{s}}| - k_{\mathrm{s}}S_{\mathrm{s}}^2 - \xi_{\mathrm{f}}\|\boldsymbol{S}_{\mathrm{f}}\| - k_{\mathrm{f}}\|\boldsymbol{S}_{\mathrm{f}}\|^2 < 0 \end{aligned} \tag{32}$$

where $\|\cdot\|$ denotes the Euclidean norm.

It can be concluded the stability condition is satisfied, and thus the closed-loop system is asymptotically stable.

This completes the proof. □

In order to improve chattering phenomenon of the SMC, the sgn($\cdot$) function is replaced by Euclidean norm, which resulting the eventual SMC law as follows

$$\begin{bmatrix} u_{\mathrm{d}} \\ u_{\mathrm{q}} \end{bmatrix} = \int_0^t \frac{JR_{\mathrm{s}}}{K_{\mathrm{T}}} \begin{bmatrix} -\frac{p_{\mathrm{n}}L_{\mathrm{s}}}{R_{\mathrm{s}}}\omega_{\mathrm{m}} \\ 1 \end{bmatrix} \left(c\dot{e}_{\mathrm{w}} + \ddot{\omega}_{\mathrm{m}}^* - A_{\mathrm{s}}\dot{\omega}_{\mathrm{m}} + \xi_{\mathrm{s}}\frac{S_{\mathrm{s}}}{\|S_{\mathrm{s}}\|^2} + k_{\mathrm{s}}S_{\mathrm{s}} \right) \mathrm{d}t - R_{\mathrm{s}}\left(\boldsymbol{A}_{\mathrm{f}}\boldsymbol{i}_{\mathrm{f}} + \xi_{\mathrm{f}}\frac{\boldsymbol{S}_{\mathrm{f}}}{\|\boldsymbol{S}_{\mathrm{f}}\|^2} + k_{\mathrm{f}}\boldsymbol{S}_{\mathrm{f}} \right) \tag{33}$$

Remark 5. *The robustness of the SMC strategy is guaranteed by introducing the sgn(·) function term into the control law, which unavoidably causes the chattering phenomenon [26]. In this study, the Euclidean norm is incorporated into the eventual control law (33), such resulting suppressing the inherent chattering phenomenon caused by sgn(·) function, while the anti-disturbance performance of the controlled system is still maintained. For the subsequent actual implementation [27], the modified revision of* $\boldsymbol{S}/(\|\boldsymbol{S}\| + 0.001)$ *should be recommended to replace the* $\boldsymbol{S}/\|\boldsymbol{S}\|$*, where a small positive constant is added in the denominator. In addition, it should be emphasized that the high quality differential signals provided by TD (22) will be employed in the designed controller (33), which can significantly improve the system performance.*

As a result, the corresponding whole schematic block diagram of dual-time-scale SMC for a surface-mounted PMSM drive system is shown as Figure 1. First of all, based on the velocity tracking error e_{w} between the reference velocity value ω_{m}^* and the actual feedback velocity ω_{m}, the S-SMC (20) generates the slow variable components $\boldsymbol{u}_{\mathrm{s}}$ (u_{ds} and u_{qs}). Meanwhile, according to the famous Clark and Park transformation equations (θ_{e} is the spatial angle of rotor flux linkage vector, where a mod operation is usually involved with respect to 2π), the three-phase symmetrical currents i_{A}, i_{B} and i_{C} can be equivalently converted to d and q axes currents i_{d} and i_{q}. Incorporating the ω_{m} and $\boldsymbol{u}_{\mathrm{s}}$ into the obtained i_{d} and i_{q}, the fast variable current components $\boldsymbol{i}_{\mathrm{f}}$ (i_{df} and i_{qf}) can be exactly extracted, which will be adopted in F-SMC (28). Therefore, the eventual SMC law $\boldsymbol{u}$ (u_{d} and u_{q}) can be synthesized by combining $\boldsymbol{u}_{\mathrm{s}}$ and $\boldsymbol{u}_{\mathrm{f}}$ (u_{df} and u_{qf}), which are subsequently employed to generate the modulation waves u_α and u_β (through the Park inverse transformation) for space vector pulse width modulation (SVPWM) component. In the last, the corresponding a series of digital pulse (constant amplitude with unequal width) signals are transmitted to the three-phase full-bridge inverter, such generating the three-phase symmetrical voltages for the surface-mounted PMSM. To this end, the closed-loop control of the speed regulation system is performed by employing the eventual SMC law (33).

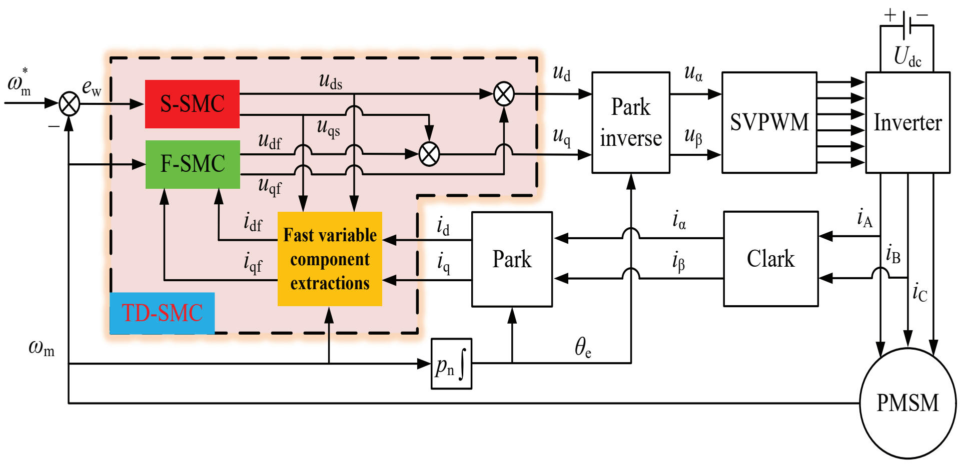

Figure 1. The schematic block diagram of dual-time-scale SMC for a PMSM drive system.

For the above mentioned schematic block diagram (shown as Figure 1), we can identify it as "TD-SMC", because there involves the TD to generate the differential signal. On the other hand, the standard double closed-loop cascade vector control framework (named by "SMC") is shown as Figure 2, which is comprised by the outer SMC speed loop and inner PI current loop. The different structures will be employed to obtain the comparative speed performance.

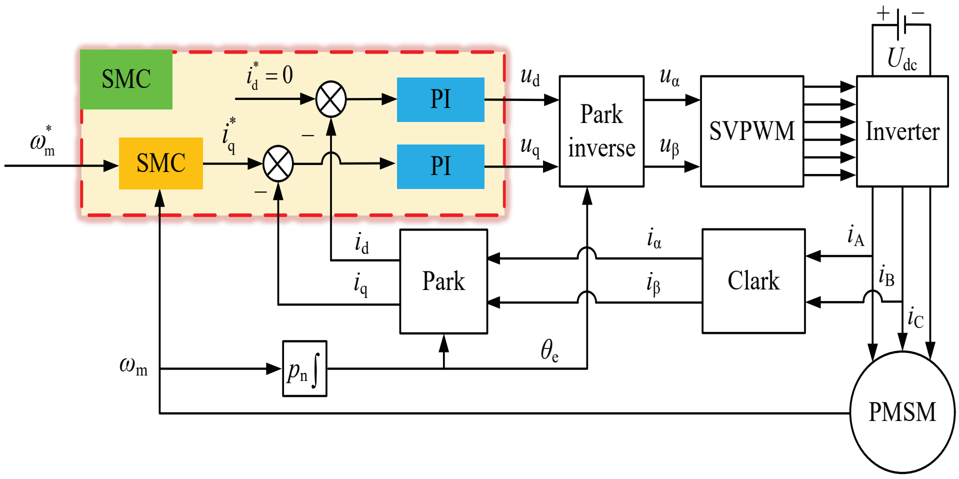

Figure 2. The double closed-loop cascade vector control framework.

Remark 6. *This study proposes the dual-time-scale SMC (symbolized by Figure 1) for a PMSM speed regulation system, which is inspired by the fast slow response characteristic of a surface-mounted PMSM. As a result, the non-cascade control structure that different from the traditional vector control strategy (namely, the Figure 2) is exhibited in the motor community. Moreover, the advantages and effectiveness of the presented alternative control framework are demonstrated by the following comparison results.*

4. Simulation Results

In this section, a surface-mounted PMSM is considered to demonstrate the effectiveness and advantages of the proposed approach, whose specification parameter values are listed in Table 1. When the uncertainties and disturbances are not taken into account in the electrical dynamics (1) and mechanical Equation (2), their corresponding transfer functions for the nominal systems can be characterized by a classical inertia element with the individual time constants. According to Table 1, we can calculate that $T_c = 5.217 \times 10^{-3}$ and $T_s = 5.8$, respectively, which illustrate the relationship (5), thus resulting the dual-time-scale characteristic of the surface-mounted PMSM drive system.

Table 1. Specification parameters of a surface-mounted PMSM.

Symbol	Value	Unit
R_s	2.875	Ω
L_s	15	mH
ψ_f	0.15	Wb
U_n (Rated voltage)	220	V
J	0.029	kg·m^2
F	5×10^{-3}	–
p_n	4	–

In addition, the DC-link capacitor voltage for the voltage source inverter and the pulse width modulation (PWM) frequency are set as $U_{dc} = U_n \times \sqrt{2}$V and $f_{PWM} = 10\,$kHz, respectively. Because there has the integration operation in the S-SMC (20), it is reasonable to set the output saturation values as $\pm 0.9 \times U_n$. In addition, the other design parameters of the constructed TD (22) and the eventual SMC (33) are listed in Table 2.

Table 2. Design parameters of the constructed TD and the eventual SMC.

T_o	h	r	c	ξ_s	k_s	ξ_f	k_f
1×10^{-6}	$10 \times T_o$	1×10^4	1×10^3	5	100	1.5	50

For the sake of illustrating the effectiveness of the presented approaches, one can firstly give the reference velocity value ω_m^* as a step signal, which changes from 40 rad/s to 90 rad/s at 0.3 s. In order to generating the second-order differential signal $\ddot{\omega}_m^*$, which will be incorporated into the designed S-SMC (20), a nested TD (22) structure is employed in Figure 1. As a result, its evolution together with the first-order time-derivative signal $\dot{\omega}_m^*$ are shown as Figure 3, which reveal that the proposed TD can produce the high quality differential signals with the perfect noise filtering performance.

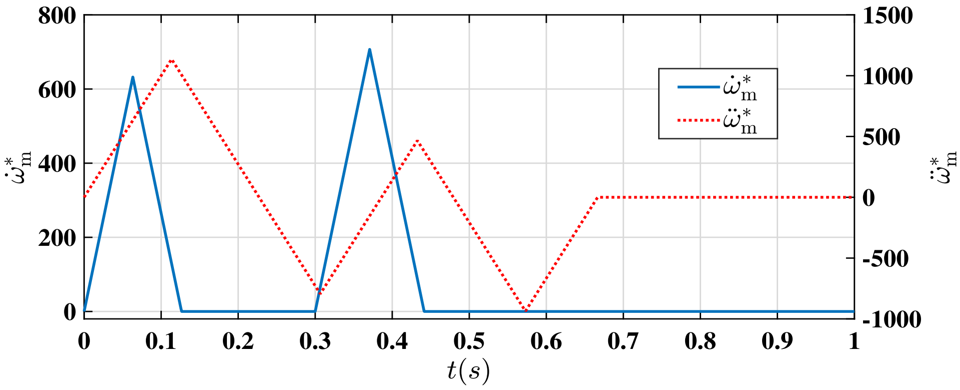

Figure 3. The evolution curves of differential signals.

In order to the implement the traditional double closed-loop cascade vector control framework (shown as Figure 2), we can firstly deign the controller for the out speed loop, which resulting the following SMC law:

$$\frac{\mathrm{d}}{\mathrm{d}t} i_q^* = \frac{J}{K_T}[250\dot{e}_w + 5\mathrm{sgn}(S) + 30S] + \frac{F}{K_T}\dot{\omega} \tag{34}$$

where the sliding mode surface is constructed as $S = 250e_w + \dot{e}_w$. At the same time, the PI controller is adopted for the inner current loop, where the gain parameters are determined as $K_P = 50$ and $K_I = 100$, respectively. In addition, the saturation values for the outer and inner loops are set as ± 30 A and ± 200 V, respectively. The corresponding comparative velocity tracking performances are shown as Figures 4 and 5.

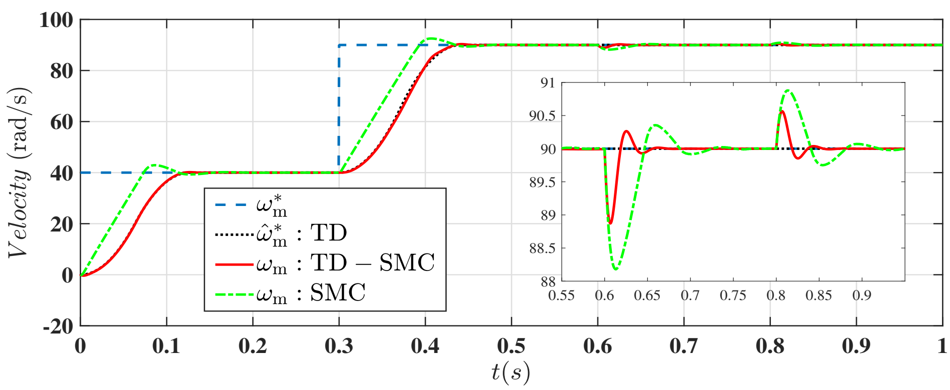

Figure 4. The reference velocity signal with its corresponding estimation and response values.

After the eventual SMC (33) is employed, the velocity response ω_m and its corresponding TD-based estimation value $\hat{\omega}_m^*$ are shown as Figure 4. From the Figure 4, it can be seen that the presented TD (22) can generate a favourable transition dynamic, while the feedback velocity response is smooth without small overshoot.

Meanwhile, the velocity tracking error e_w is also exhibited as Figure 5, which is used to further analyze the tracking performance.

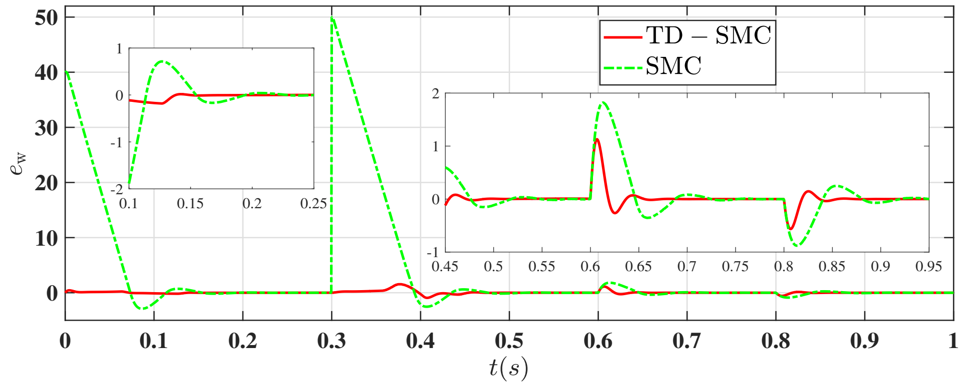

Figure 5. The characteristic curves of velocity tracking error e_w.

Furthermore, in order to demonstrate the speed regulation system robustness against the external disturbance T_m, an initial load torque value 5 N·m is added. In addition, a variable step disturbance that suddenly varies from 5 N·m to 15 N·m at 0.6 s, and then decreasing to 10 N·m at 0.8 s is employed. According to some performance indexes, the detailed comparisons can also be found in Table 3.

Table 3. Speed response performance comparisons.

Index	TD-SMC	SMC
Response time (0 → 40 rad/s)	0.16 s	0.25 s
Overshoot (0 → 40 rad/s)	0.25 rad/s	3 rad/s
Response time (40 rad/s → 90 rad/s)	0.18 s	0.24 s
Overshoot (40 rad/s → 90 rad/s)	0.4 rad/s	2.6 rad/s
Recovering time (5 N·m → 15 N·m)	0.07 s	0.15 s
Velocity fluctuation (5 N·m → 15 N·m)	1.2 rad/s	1.9 rad/s
Recovering time (15 N·m → 10 N·m)	0.08 s	0.17 s
Velocity fluctuation (15 N·m → 10 N·m)	0.6 rad/s	0.9 rad/s

It can be concluded form Figures 4 and 5 and Table 3 that the actual feedback velocity ω_m can quickly recover to its reference value $\hat{\omega}_m^*$ in the presence of variable external disturbances, while the more satisfactory tracking performance and anti-disturbance ability are presented by comparing with the conventional SMC strategy. In addition, the imposed torque, electromagnetic torque T_e with q axis stator current i_q are shown as Figure 6, respectively. It can be concluded that the torque output is directly proportional to i_q with the electromagnetic torque coefficient K_T, while it can accurately balance the external torque T_m and viscous friction effect $F\omega_m$, simultaneously.

Finally, for the sake of exploring the current transient response performance, the three-phase current signals are shown as Figure 7. It can be seen that the three-phase currents i_A, i_B and i_C are completely symmetrical, while the electrical angle difference is $2\pi/3$ for each other.

Benefitting from the excellent adjustment capacity, it can be concluded from Figures 4–6 that the presented dual-time-scale SMC for PMSM regulation system can precisely track the reference velocity signal and actively suppress the disturbances, simultaneously. It can be concluded that the closed-loop system under the eventual SMC (33) has strong robustness against the external disturbances, where the Euclidean norm rather than sgn(·) function is employed to improve the inherent chattering phenomenon. Meanwhile, it is worth mentioning that the tracking performance is characterized by quick response speeds, small overshoot and steady-state error, etc, where the velocity fluctuations are within ±1.5 rad/s in the presence of external disturbances.

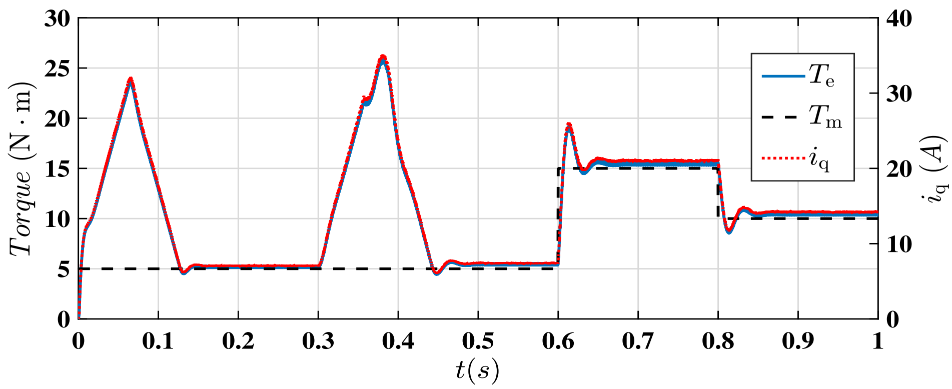

Figure 6. The evolution curves of T_m, T_e and i_q.

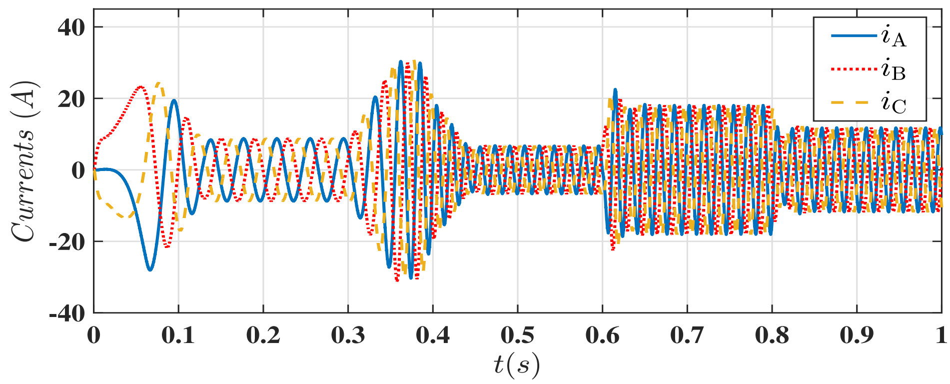

Figure 7. The three-phase current signals.

It is well-known that the stator resistance of motor winding will change along with operation temperature, thus it is recommended to research the robustness against parametric perturbations. To this end, we employ different stator resistance values for the surface-mounted PMSM listed in Table 1, and adopt the above mentioned proposed control strategy with the same R_s. On the other hand, the initial reference velocity ω_m^* value 50 rad/s is given, while a sudden 10 N·m load torque is added at 0.3 s, thus resulting the corresponding velocity response curves shown as Figure 8. It can be concluded that the presented approach has certain robustness against the parametric variation of stator resistance. The more rigorous and comprehensive research on parametric perturbations will be considered in our future work.

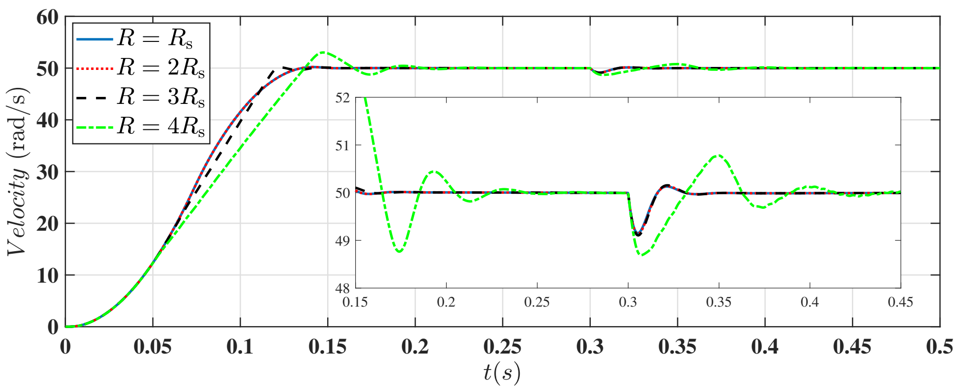

Figure 8. The evolution curves of velocity response with different stator resistance values.

5. Conclusions

This paper has investigated the problem of dual-time-scale SMC for the surface-mounted PMSMs with disturbances. A quasi-steady-state theory-based decomposing, an optimal control synthesis function-based TD and a novel SMC method have been exhibited in details, respectively. By demonstrating the eventually synthesized control law, it can be concluded that the obtained servo drive system possesses strong anti-disturbance performance. In addition, the velocity tracking performance has the characteristic of rapid response dynamics, small overshoot and steady-state error, and so on. Our future work will concentrate on the disturbance observer-based SMC, where will involve the design and analysis of disturbance observer, such resulting the estimation compensation values of parametric uncertainties and external disturbances, simultaneously. In addition, the experimental implementation will be performed to demonstrate the stability and effectiveness when considering the interrupt execution period, etc.

Author Contributions: This is a joint work and the authors were in charge of their expertise and capability: Z.C. for investigation and analysis; H.Y. for validation and revision; S.M. for methodology; M.A. for writing and revision; C.Y. for manuscript revision; F.F.M.E.-S. for data analysis. All authors have read and agreed to the published version of the manuscript.

Funding: This work were supported by the National Natural Science Foundation of China under Grant 41576096, 42176211, Fundamental Research Funds for the Central Universities under Grant 3216002104D, and Postgraduate Research & Practice Innovation Program of Jiangsu Province under Grant SJCX20_0013.

Acknowledgments: The authors would like to express their gratitude to all those who helped them during the writing of this paper. And the authors would like to thank the reviewers for their valuable comments and suggestions.

Conflicts of Interest: The authors declare no conflict of interest.

References

1. Pei, W.H.; Zhang, Q.; Li, Y.J. Efficiency Optimization Strategy of Permanent Magnet Synchronous Motor for Electric Vehicles Based on Energy Balance. *Symmetry* **2022**, *14*, 164. [CrossRef]
2. Wang, Y.; Yu, H.T.; Liu, Y.L. Speed-Current Single-Loop Control With Overcurrent Protection for PMSM Based on Time-Varying Nonlinear Disturbance Observer. *IEEE Trans. Ind. Electron.* **2022**, *69*, 179–189. [CrossRef]
3. Che, Z.; Yu, H.; Mobayen, S.; Ali, M.; Yang, C.; Bartoszewicz, A. An Improved Extended State Observer-Based Composite Nonlinear Control for Permanent Magnet Synchronous Motor Speed Regulation Systems. *Energies* **2022**, *15*, 5699. [CrossRef]
4. Jung, J.W.; Leu, V.Q.; Do, T.D.; Kim, E.-K.; Choi, H.H. Adaptive PID Speed Control Design for Permanent Magnet Synchronous Motor Drives. *IEEE Trans. Power Electron.* **2015**, *30*, 900–908. [CrossRef]
5. Choi, J.; Nam, K.; Bottsov, A.A.; Pyrkin, A.; Ortega, R. Robust Adaptive Sensorless Control for Permanent Magnet Synchronous Motors. *IEEE Trans. Power Electron.* **2017**, *32*, 3989–3997. [CrossRef]
6. Mynar, Z.; Vesely, L.; Vaclavek, P. PMSM Model Predictive Control with Field-Weakening Implementation. *IEEE Trans. Ind. Electron.* **2016**, *63*, 5156–5166. [CrossRef]
7. Mobayen, S.; Mostafavi, S.; Fekih, A. Non-Singular Fast Terminal Sliding Mode Control With Disturbance Observer for Underactuated Robotic Manipulators. *IEEE Access* **2020**, *8*, 198067–198077. [CrossRef]
8. Mofid, O.; Mobayen, S.; Wong, W.K. Adaptive Terminal Sliding Mode Control for Attitude and Position Tracking Control of Quadrotor UAVs in the Existence of External Disturbance. *IEEE Access* **2021**, *9*, 3428–3440. [CrossRef]
9. Nguyen, Q.D.; Giap, V.N.; Tran, V.H.; Pham, D.-H.; Huang, S.-C. A Novel Disturbance Rejection Method Based on Robust Sliding Mode Control for the Secure Communication of Chaos-Based System. *Symmetry* **2022**, *14*, 1668. [CrossRef]
10. Li, S.H.; Zong, K.; Liu, H.X. A Composite Speed Controller Based on A Second-Order Model of Permanent Magnet Synchronous Motor System. *Trans. Inst. Meas. Control* **2011**, *33*, 522–541.
11. Wang, H.; Li, S.; Lan, Q.; Zhao, Z.; Zhou, X. Continuous terminal sliding mode control with extended state observer for PMSM speed regulation system. *Trans. Inst. Meas. Control* **2017**, *39*, 1195–1204. [CrossRef]
12. Xu, W.; Jiang, Y.J.; Mu, C.X. Novel Composite Sliding Mode Control for PMSM Drive System Based on Disturbance Observer. *IEEE Trans. Appl. Supercond.* **2016**, *26*, 1–5. [CrossRef]
13. Wang, H.M.; Li, S.H.; Yang, J.; Zhou, X.P. Continuous Sliding Mode Control for Permanent Magnet Synchronous Motor Speed Regulation Systems Under Time-Varying Disturbances. *J. Power Electron.* **2016**, *16*, 1324–1335. [CrossRef]
14. Zhang, X.G.; Sun, L.Z.; Zhao, K.; Sun, L. Nonlinear Speed Control for PMSM System Using Sliding-Mode Control and Disturbance Compensation Technique. *IEEE Trans. Power Electron.* **2013**, *28*, 1358–1365. [CrossRef]

15. Rayguru, M.M.; Mohan, R.E.; Parween, R.; Yi, L.; Le, A.V.; Roy, S. An Output Feedback Based Robust Saturated Controller Design for Pavement Sweeping Self-Reconfigurable Robot. *IEEE/ASME Trans. Mechatronics* **2021**, *26*, 1236–1247. [CrossRef]
16. Liu, X.; Yu, H.; Yu, J.; Zhao, L. Combined Speed and Current Terminal Sliding Mode Control with Nonlinear Disturbance Observer for PMSM Drive. *IEEE Access* **2018**, *6*, 29594–29601. [CrossRef]
17. Li, T.; Liu, X.D. Model-Free Non-Cascade Integral Sliding Mode Control of Permanent Magnet Synchronous Motor Drive with a Fast Reaching Law. *Symmetry* **2021**, *13*, 1680. [CrossRef]
18. Son, Y.I.; Kim, I.H.; Choi, D.S.; Shim, H. Robust Cascade Control of Electric Motor Drives Using Dual Reduced-Order PI Observer. *IEEE Trans. Ind. Electron.* **2015**, *62*, 3672–3682. [CrossRef]
19. Rayguru, M.M.; Dey, B.S.; Kar, I.N. Output Feedback for Contraction of Nonlinear Singularly Perturbed Systems. *Int. J. Control* **2021**, *95*, 2199–2210. [CrossRef]
20. Munje, R.; Gu, D.; Desai, R.; Patre, B.; Zhang, W. Observer-Based Spatial Control of Advanced Heavy Water Reactor Using Time-Scale Decoupling. *IEEE Trans. Nucl. Sci.* **2018**, *65*, 2756–2766. [CrossRef]
21. Pan, Y.; Li, X.; Wang, H.; Yu, H. Continuous Sliding Mode Control of Compliant Robot Arms: A Singularly Perturbed Approach. *Mechatronics* **2018**, *52*, 127–134. [CrossRef]
22. Zhou, L.N.; Shen, L.P.; Yang, C.Y. Disturbance-Observer Based Sliding Mode Control for Fuzzy Singularly Perturbed Systems. *J. Intell. Fuzzy Syst.* **2019**, *37*, 1055–1064. [CrossRef]
23. Nguyen, T.; Su, W.C.; Gajic, Z. Variable Structure Control for Singularly Perturbed Linear Continuous Systems with Matched Disturbances. *IEEE Trans. Autom. Control* **2012**, *57*, 777–783. [CrossRef]
24. Su, Y.X.; Zheng, C.H.; Duan, B.Y. Automatic Disturbances Rejection Controller for Precise Motion Control of Permanent-Magnet Synchronous Motors. *IEEE Trans. Ind. Electron.* **2005**, *52*, 814–823. [CrossRef]
25. Han, J.Q. *Active Disturbance Rejection Control Technique*; National Defense Industry Press: Beijing, China, 2008; pp. 197–270.
26. Truc, L.N.; Vu, L.A.; Thoan, T.V.; Thanh, B.T.; Nguyen, T.L. Adaptive Sliding Mode Control Anticipating Proportional Degradation of Actuator Torque in Uncertain Serial Industrial Robots. *Symmetry* **2022**, 14, 957. [CrossRef]
27. Zhang, J.H.; Liu, X.W.; Xia, Y.Q. Disturbance Observer-Based Integral Sliding-Mode Control for Systems With Mismatched Disturbances. *IEEE Trans. Ind. Electron.* **2016,** *63*, 7040–7048. [CrossRef]